https://bjas.journals.ekb.eg/ engineering sciences

A Wideband circularly polarized MIMO Antenna for 5G Millimeter Wave Applications

Rehab I. Nawar, Abdelhady M. Abdelhady and Ashraf Y. Hassan.

Electrical Engineering Dept., Benha Faculty of Engineering, Benha University, Benha, Egypt.

Email: rehab.nawar@bhit.bu.edu.eg

Abstract

This study presents a broadband, circularly polarized millimeter-wave four-port multiple-input-multiple-output (MIMO) antenna design featuring enhanced performance attributes. The MIMO antenna structure comprises four monopole elements with a common ground. Simulated on a Rogers RT5880 substrate with dimensions 25 mm \times 31 mm and a thickness of 1.575 mm, the antenna demonstrates excellent characteristics. The MIMO achieves a high impedance bandwidth of 21.5 to 45 GHz, a wide 3-dB axial ratio bandwidth (ARBW) of 23.5 to 30.7 GHz, covering critical frequencies such as 28 GHz, and exhibits high isolation with S21 < -20 dBi. The axial ratio bandwidth (ARBW) and peak gain (8.5 dBi) are enhanced, and the MIMO performance is greatly improved by adding parasitic elements between the MIMO elements. Massive MIMO can be constructed using an eight-port from the same monopole antenna. The compact size and simplified fabrication process make this antenna design a promising solution for demanding ultra-wideband communication scenarios and 5G millimeter-wave applications.

Keywords Wideband, Circularly Polarized (CP), MIMO, Gain, and 5G Millimeter Wave Applications.

1. Introduction

As wireless communication technologies advance rapidly, the importance of fifth-generation (5G) technology is increasingly recognized for its highspeed data transfer rates, low latency, and capacity to handle high traffic volumes. The 5G spectrum is divided into two main parts: the Sub-6 GHz band (450-6000 MHz) and the millimeter-wave band (24.25–52.6 GHz). With the Sub-6 GHz band facing spectrum resource depletion, attention is shifting towards utilizing the millimeter-wave (mm-Wave) band. The International Telecommunication Union has identified new radio (NR) bands for International Mobile Telecommunication (IMT), FR-II (24.25 GHz to 52.6 GHz) channels such as n-258 (24.25-27.5 GHz) and n-261 (28.35 GHz) [1]. Leading countries in 5G research implementation, such as Korea, the United States, Japan, the United Kingdom, China, Canada, and the European Union, are utilizing the mmWave spectrum sub-range (24.2-29.5 GHz) for 5G communication[2]. The millimeter-wave spectrum excels in providing high-capacity, low-latency connections in dense urban areas and specific hotspots, enabling ultra-fast speeds, smaller antenna size, high-resolution, and high data rates, and supporting applications like HD video applications [3], satellite communication, radar applications [4], medical application [5, 6], internet of things[7], and virtual reality. Despite its advantages, millimeterwave transmissions are susceptible to atmospheric attenuation from fog, rain [8], gaseous losses, and propagation path losses [9, 10]. To address these challenges, high-gain, highly directive antennas are

commonly employed in millimeter-wave communications. These antennas concentrate the transmitted signal in specific directions, enhancing signal strength and optimizing link quality. Broadband circular polarization (CP) antenna arrays are becoming increasingly attractive as solutions to this issue.

print: ISSN 2356-9751

online: ISSN 2356-976x

Circular polarization (CP) is a multipurpose technology that works well in bad weather, successfully stops multipath fading, and preserves signal integrity in difficult propagation environments. Additionally, it reduces the criticality of receiving antenna orientation by providing wireless systems with adequate mobility. CP antennas can be designed in several ways, including monopoles [11], aperture antennas [12, 13], patch antennas [14–16], etc.

MIMO technology allows simultaneous use of multiple antennas, and is crucial for 5G communication due to enhanced low latency, high data rates, channel capacity, quality, spectrum efficiency, and reduced multiple fading [17-20] As reported in [21–24]literature, these MIMO antennas function well, showing low mutual coupling, but they are linearly polarized and have low gain characteristics (gain < 8 dBic). Therefore, using circularly polarized Multiple-Input Multiple-Output (MIMO) antennas offers a significant benefit in overcoming the drawbacks of millimeter-wave (mmWave) technology. Additionally, wideband (UWB) antennas are known to offer faster data rates [25-27] and enhance performance in the millimeter-wave spectrum [28].

The literature review indicates that few studies have been conducted on designing CP MIMO antennas in the 5G frequency bands [29–35]. Research suggests that designing CP MIMO antennas for 5G frequency bands is challenging due to their small size and the limited space available for connectors. Fabry-Pérot CP antennas offer high gain and isolation but also face complications, including large antenna profiles, mechanical issues, and a complex design [29-31] due to the air gap between the superstrate and the antenna. The concept of frequency selective surfaces (FSS) and multiple layered substrates are challenging to implement and unsuitable for realworld mass manufacturing. Circularly Polarized (CP) MIMO can also be accomplished by using Dielectric Resonator Antennas (DRA), as described in references [32, 33]. Nevertheless, this method usually makes the system more complex. Metasurfaces, two-dimensional metamaterials, are combined with radiators for wideband AR and gain enhancement, maintaining the antenna's low profile, but with design complexities and poor mechanical properties because of added air gap either above [34] or below [35].

In this paper, a low-profile CP MIMO antenna is required because none of the published antennas in the literature provide broad bandwidth, CP, and MIMO properties in a single-layer design. In light of the aforementioned considerations, a single-layer CP antenna based on a monopole element and its MIMO characterization is recommended for 5G Millimeter Wave Applications. This introduces a design for a wideband Circularly Polarized (CP) monopole antenna that covers the desired frequency band (21 to 45 GHz). Subsequently, four MIMO elements are constructed from monopole antennas to provide maximum isolation between the elements and enhance gain by incorporating parasitic elements between them. Additionally, wideband Axial Ratio performance is achieved. Using the CST Microwave Studio suite, the MIMO antenna is designed on a Rogers RT5880 substrate (Er= 2.2) that has a thickness of 1.575 mm. High isolation between elements resulted in |S21| < -20 dB. The peak gain is 8.5 dBi, with 70.6% IBW and 27% ARBW. We go into the details in the sections that follow.

2. Materials and Methods

The antenna design process began with the development of a circular patch element, specifically designed for operation in the mmWave spectrum and featuring circular polarization.

Initially, modifications were made to the circular patch by implementing strategic cuts, while a partial ground structure was introduced to achieve a broad operational bandwidth.

Subsequently, a MIMO configuration was constructed, comprising four interconnected elements sharing a common ground. To enhance

performance metrics such as gain and axial ratio bandwidth, parasitic elements were strategically integrated into the MIMO structure.

Building upon this foundation, an eight-element MIMO system was engineered by modifying the ground plane of each individual element. These adjustments were instrumental in optimizing the efficiency of the MIMO setup.

The entire design process was executed on a Rogers RT5880 substrate (Er=2.2), with simulation and analysis conducted using the CST Studio Suite software suite. The results obtained through these simulations provided valuable insights into the performance characteristics and capabilities of the developed antenna configurations. In the subsection that follows, this will be clarified.

2.1 Design a Wideband CP Monopole

Figure 1 illustrates the proposed broadband CP antenna on a Rogers RT5880 dielectric substrate that is 1.575 mm thick, has a relative permittivity of 2.2, and sizes 15 x 12 mm² with thickness of 1.575 mm. A feedline monopole antenna with a 50-ohm microstrip transmission. Table 1 displays the final parameters of the suggested antenna, which were optimized with the CST microwave studio suite.

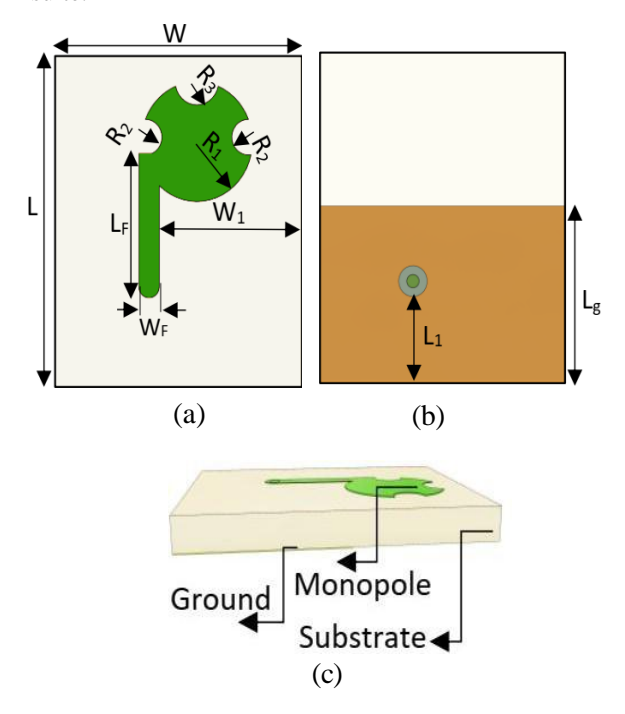


Fig. 1 The suggested antenna's layout (a) top view, (b) bottom view, and (c) 3D view

Table 1 Designed single antenna's dimensions

Parameter	Value	Parameter	Value
L	15	R_3	1.05
W	12	W1	6.9
R_1	2.7	L1	4.05
R_2	0.8	L_{g}	8
$L_{\rm F}$	6.5	\mathbf{W}_{f}	1

The improved monopole's optimized schematic is depicted in Figure 1, where it is printed on the Rogers RT5880 substrate's upper metallic layer, as seen in Figure 1(a). The parametric research in the Result section shows that the redesigned monopole is tilted ($\Theta = 44^{\circ}$) from the vertical axis to achieve broadband matching and satisfy CP performance. A 50-ohm microstrip line that ends in coaxial probe feeding (LF = 6.5 mm) supplies power to the monopole. An etching on the bottom metallic layer, where a modified ground plane is produced, is seen in Figure 1(b). These changes in Lg increase the 3-dB axial ratio bandwidth (ARBW), as shown in the Results section.

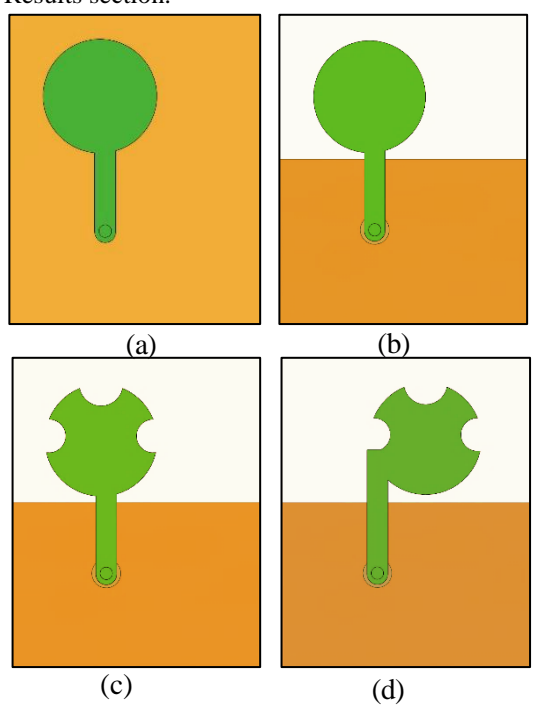


Fig. 2 Design procedures of the proposed monopole antenna with the modified ground and circle patch(a) Model-1, (b) Model-2, and (c) Model-3 (d) Final-Model

Four antennas (Modal 1-4) are analyzed to assess the design process. Figure 2 shows the detailed structure. The first step in antenna design is to start with a circular patch antenna with radius a. The radius length is determined using the equations in [36] with the full ground plane, which corresponds to Model-1, as shown in Figure 2(a). Then, as seen in Figure 2(b), it truncates the portion from the ground plane to produce Model-2. As seen in Figure 2(c), Model-3 is produced by the remaining three truncating from the edges of the patch. Figure 2(d) illustrates the final model of the suggested antenna with the patch rotated to the right at an angle of 44 degrees. This significantly improves the axial ratio band (24-30 GHz), which is crucial for creating a wideband CP antenna, and the impedance matching band (21-45 GHz), as explained in the results section.

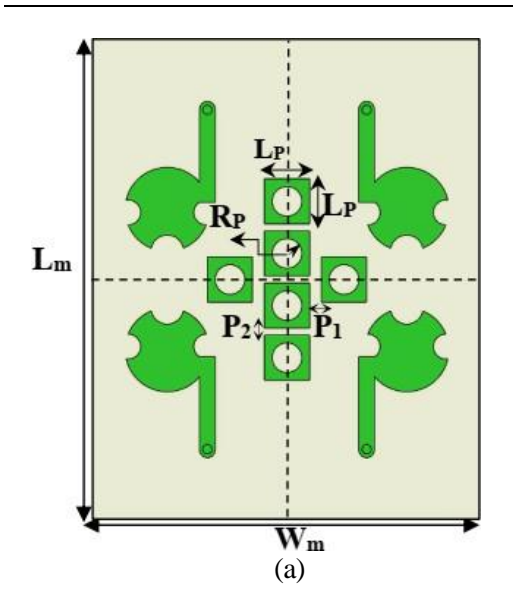
2.2 Design a Wideband CP Four-MIMO Antenna

Circularly polarized MIMO antennas are made up of four identical monopole antenna elements, as illustrated in Figure 3. Table 2 comprises the parameters of the proposed CP MIMO. The four antennas are separated by just 1 mm, or roughly 0.09 λ at the operating frequency. Four 50 Ω coaxial cables are used to feed the antenna, which enhances impedance matching. This design enables the antenna to operate with a broad axial ratio bandwidth (ARBW). To increase the gain of MIMO the parasitic element is added between the monopole antennas and their ground planes, which are joined by an I-shaped strip.

Three four-port MIMO antenna models have been created, each with a fixed inter-element spacing of D = 1mm. As seen in Figure 4(a), the first model has the monopole antennas positioned face to face with no ground plane connection. The second model, which has the ground plane connected as important in practical aspects [37], is displayed in Figure 4(b). The third model is the suggested CP MIMO, which, displayed in Figure 4(c), inserts a parasitic element in between the monopole elements. The main goal of all these adjustments is to improve the gain while maintaining ARBW to the greatest extent possible. In the final model, these objectives are ably satisfied.

Table 2 four-port MIMO dimensions

Parameter	Value	Parameter	Value
L _m	31	P ₁	0.75
\mathbf{W}_{m}	24	P_2	0.45
R_p	0.95	D	1
L_P	2.9	W_{C}	0.5



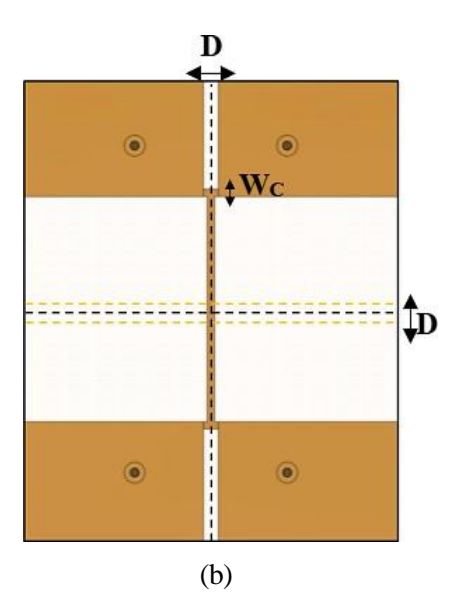
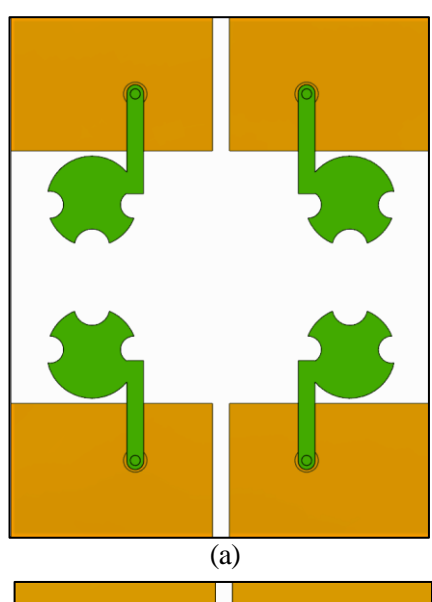
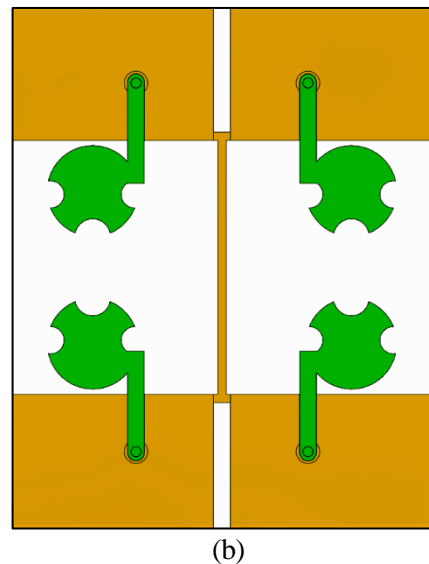


Fig. 3 Four-port CP MIMO Antenna proposal **(a)** Front side **(b)** Backside





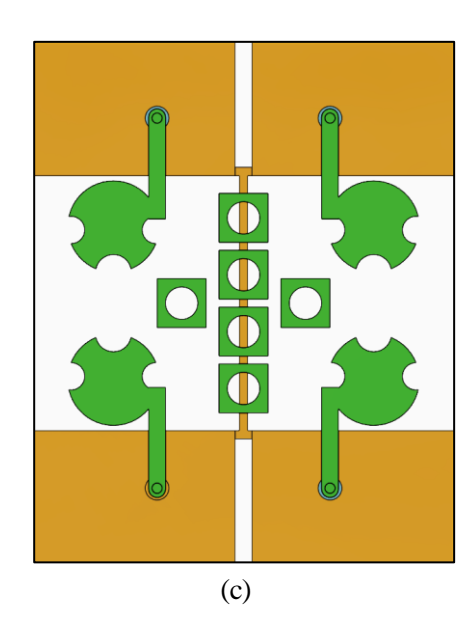


Fig. 4 Four-port CP MIMO antenna design for (a) Model 1, (b) Model 2, and (c) the suggested MIMO

2.3 Design a Wideband CP Eight-Port MIMO Antenna

Eight-port circularly polarized MIMO antennas were meticulously crafted from eight identical monopole antenna elements, with dimensions as in Figure 5. The arrangement positioned four elements above and four below in the same direction, without inter-element spacing. Notably, to optimize performance for MIMO operations, a strategic alteration of the ground plane of the monopole antenna was modified.

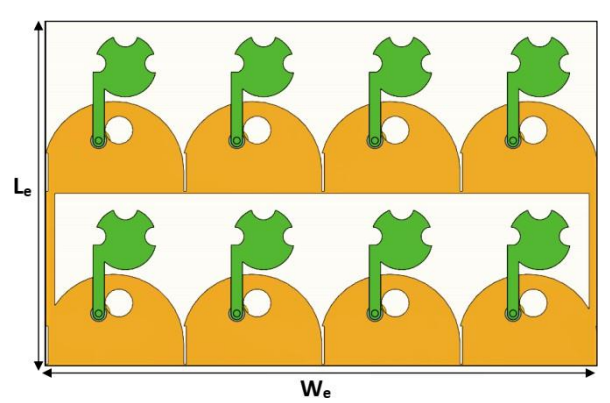


Fig. 5 proposed MIMO antenna of eight elements with L_e =30mm and W_e =48mm

3. Results and Discussion

3.1 Wideband CP Monopole Antenna

The results of the four models used to select the proposed antenna in Figure 2 in terms of bandwidth and axial ratio bandwidth (ARBW) are displayed in Figure 6. Figure 6(a) shows that the final model is the best in terms of bandwidth, extending from 21 to 45 GHz, and Figure 6(b) shows that it is the best in terms of ARBW, extending from 24.4 to 29.3 GHz. This includes the mmWave spectrum's necessary bandwidth for numerous applications.

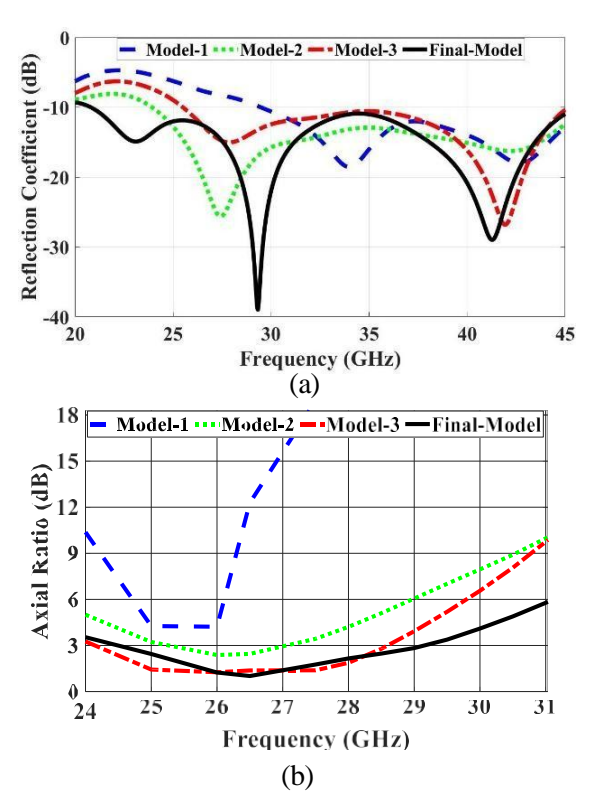
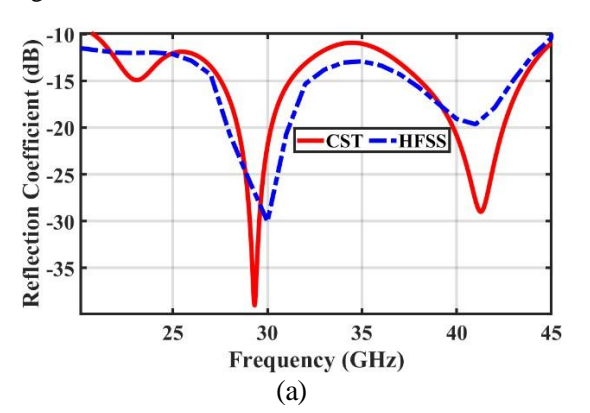


Fig. 6 Simulated S parameter and axial ratio with design steps. (a) Reflection coefficient (dB), (b) Axial Ratio (dB).

The S11 results from CST and HFSS show excellent agreement with identical bandwidth and resonant frequency in Figure 7(a). A slight frequency shift is observed in the axial ratio from HFSS, along with marginally lower values shows in Figure 7(b). The gain shows a small variation across the band as



depicted in Figure 7(c). Overall, the comparison confirms good consistency between both tools.

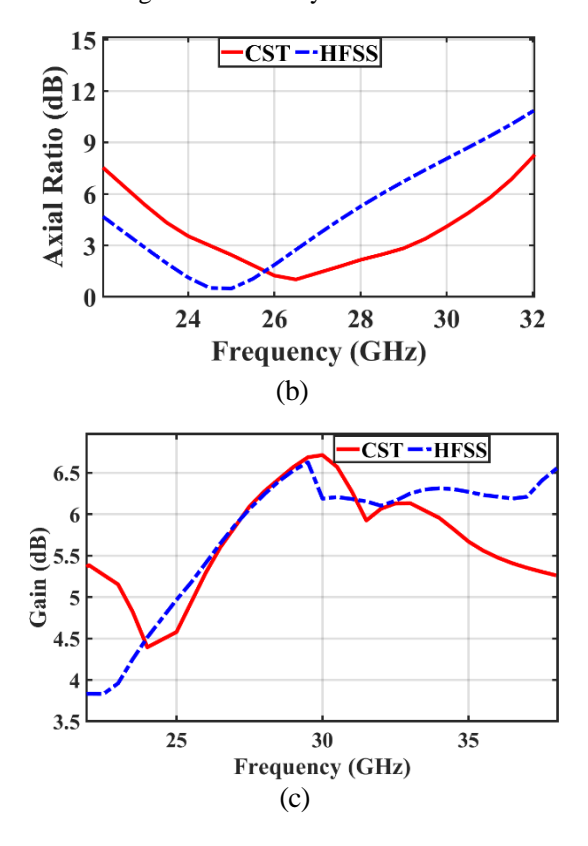


Fig. 7 Comparison of (a) S11, (b) axial ratio, and (c) gain between CST and HFSS for the proposed single-element circularly polarized antenna.

3.1.1 Parametric Analysis

This section presents a parametric analysis to examine how the geometrical parameters of the suggested antenna affect the axial ratio and reflection coefficient (S11) magnitude. Various values of L_g , L_F , and angle (Θ) are considered dominant parameters in order to comprehend the effect on bandwidth (S11) and axial ratio bandwidth.

A. Impact of L_F dimension

We find that varying the microstrip line feeding length L_F significantly impacts both the bandwidth and the axial ratio bandwidth. This is illustrated in Figure 8, where the LF length changes from 3.5 to 7.5 mm in 1 mm increments. The optimal length is 6.5 mm, resulting in a wide bandwidth as shown

Figure 8(a) and axial ratio bandwidth as depicted in Figure 8(b).

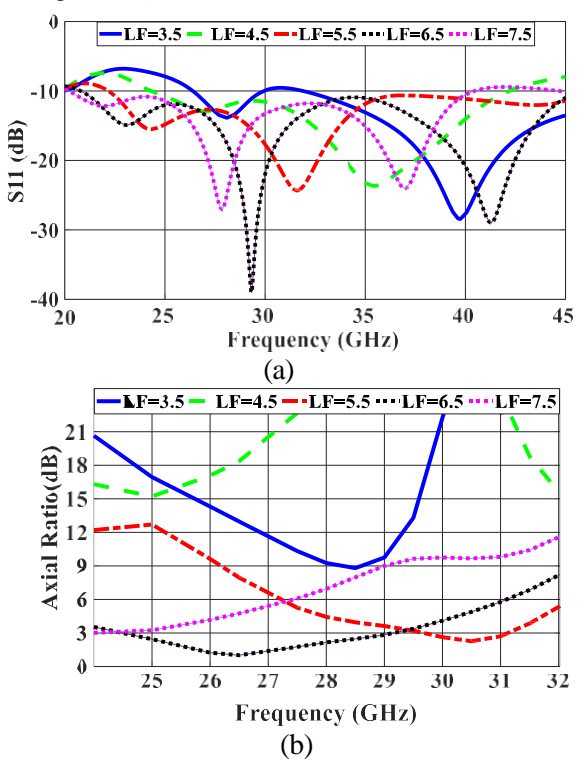


Fig. 8 Impact of the length (L_F) on (a) S11 (dB), and (b) AR (dB).

B. Impact of Lg dimension

The length of the ground plane (Lg) significantly impacts both the Axial Ratio Bandwidth (ARBW) and the bandwidth (S11), as depicted in Figure 9.

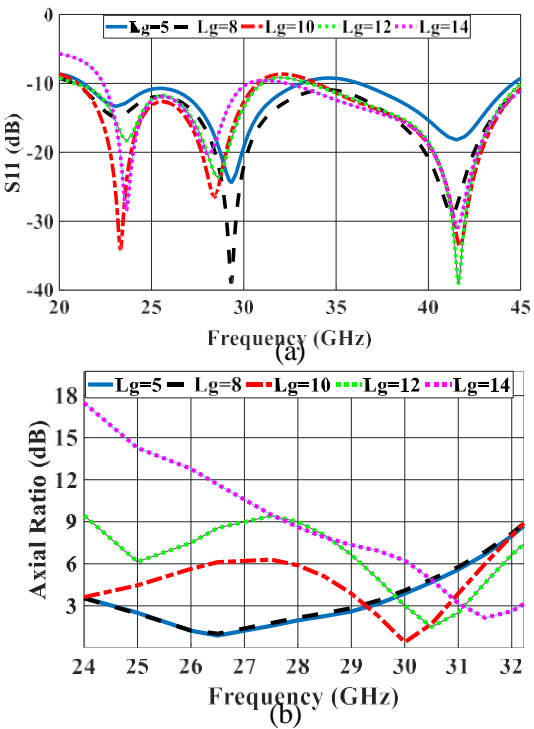


Fig. 9 Impact of the length (L_g) on (a) S11 (dB), and (b) AR (dB).

Altering the L_g length from 5 to 14mm demonstrates a notable influence on these parameters. It is observed that reducing the Lg improves the ARBW as shown Figure 9(a), with optimal results achieved at an Lg of 8mm. However, as Lg decreases beyond this point, the bandwidth begins to deteriorate as shown Figure 9(b). Therefore, the best compromise between bandwidth and ARBW is achieved at an Lg length of 8mm. This finding highlights the crucial role of the ground plane length in striking a balance between ARBW and bandwidth in antenna design.

C. Impact of theta (Θ) angle

By varying the angle (theta) representing the tilt of the modified circular patch towards the right, it is evident from Figure 10 that adjusting this angle from 0 to 50 degrees impacts the antenna performance. As theta increases, the bandwidth improves, as illustrated in Figure 10(a). This enhancement continues until reaching 44 degrees, at which point the axial ratio bandwidth begins to deteriorate. Beyond this angle, at 50 degrees as depicted in Figure 10 (b). Therefore, the optimal compromise between bandwidth and Axial Ratio Bandwidth (ARBW) is achieved at a theta angle of 44 degrees. This finding highlights the critical role of the theta angle in maximizing the performance of the antenna system, striking a balance between bandwidth and ARBW for enhanced overall efficiency.

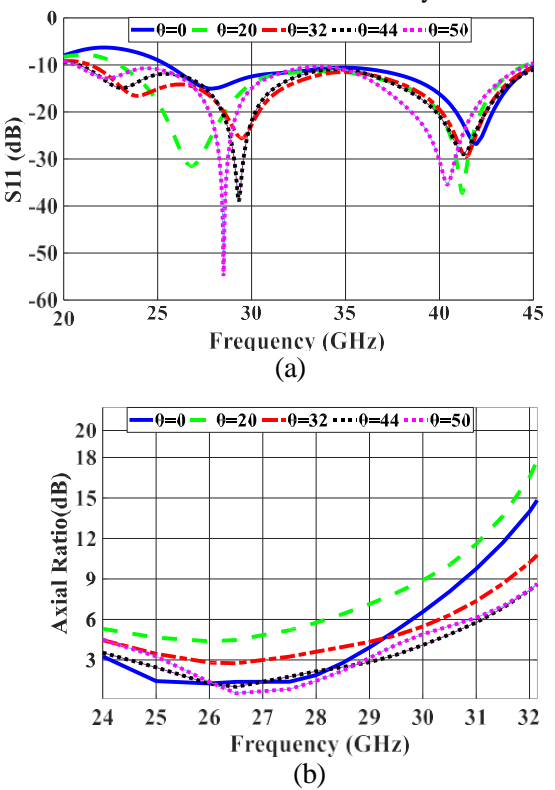
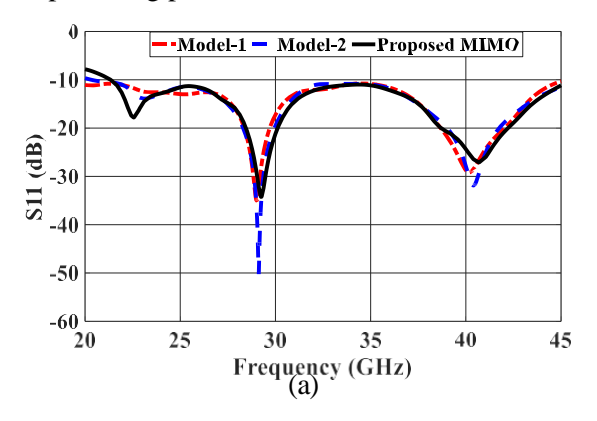


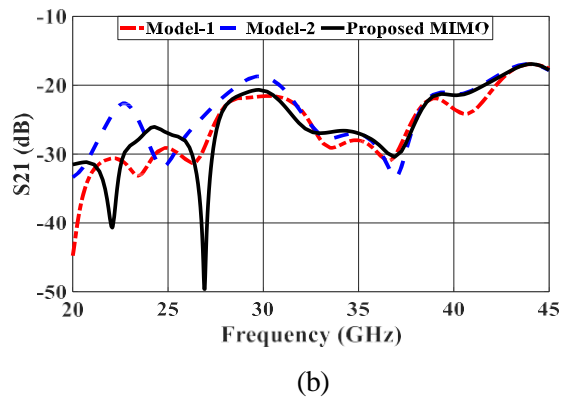
Fig. 10 Impact of theta (Θ) angle on (a) S11 (dB), and (b) AR (dB).

3.2 Wideband CP four-port MIMO

This section discusses the selection and methodology for achieving high performance for a four-port MIMO antenna. To attain optimal results, a series of steps were implemented, as illustrated in Figure 4. The most effective arrangement for the antenna elements was determined to be a configuration where each pair of elements is positioned face to face, as depicted in Figure 4(a). Subsequently, all ground connections were interlinked, a practical measure detailed in Figure 4(b), to enhance system performance.

Parasitic elements were strategically introduced between the antenna elements, culminating in the most successful model identified through the outcomes of three distinct models. Notably, the third model exhibited superior bandwidth (21.5-45 GHz) and high isolation characteristics below -20 dB in range (23 -41.5 GHz) as shown in Figure 11. This choice was validated by achieving an expanded axial ratio bandwidth ranging from 23.5 to 30.7 GHz, as depicted in Figure 12(a). Furthermore, the antenna system attained its highest gain of 8.5 dBi, as illustrated in Figure 12(b), underscoring the effectiveness of the design approach in optimizing performance metrics.





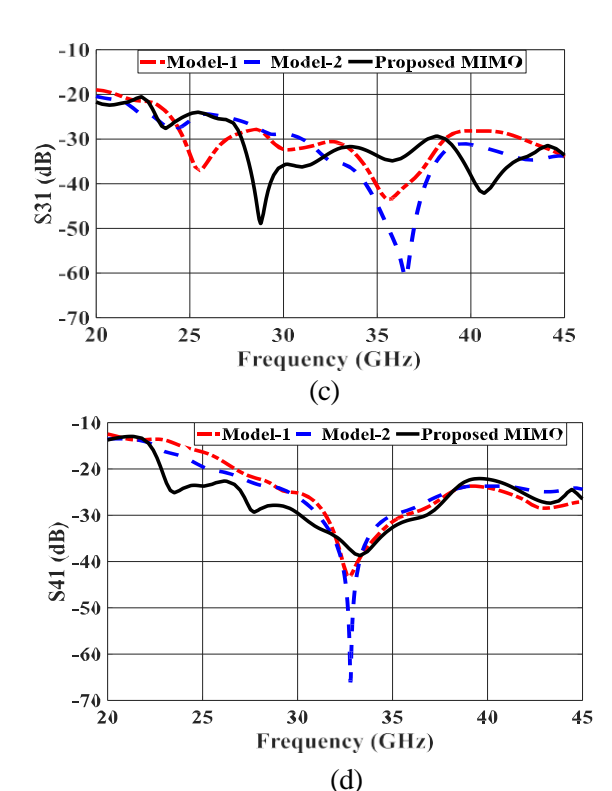


Fig. 11 Simulated performances of different design MIMO (a) S11 (dB) (b) S21 (dB) (C) S31 (dB) (d) S41 (dB)

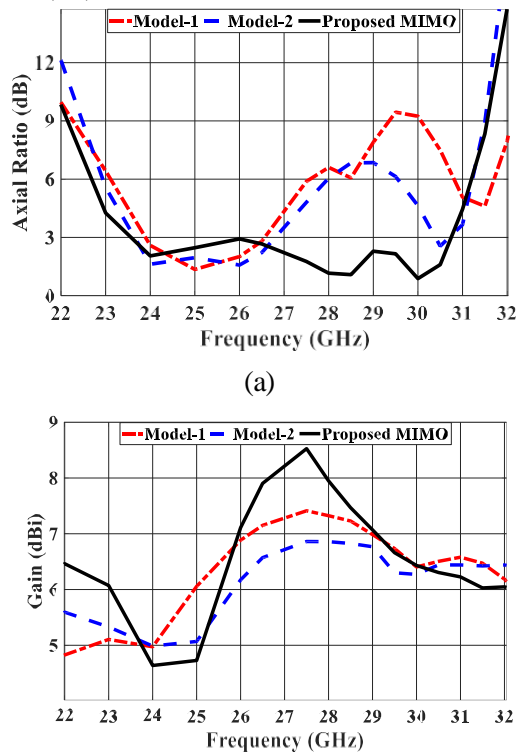
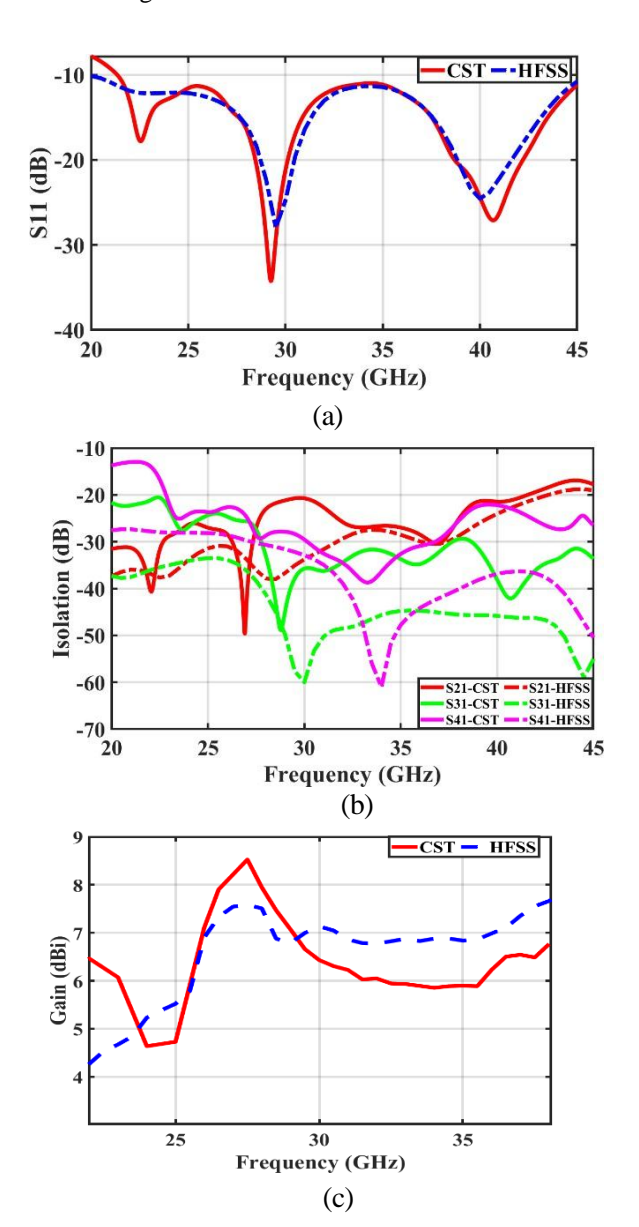


Fig. 12 Simulated performances of different design MIMO (c) Axial Ratio (dB) (b) Gain (dBi)

(b)

The S11 results from CST and HFSS are nearly identical, indicating consistent impedance matching as shown Figure 13(a). The mutual coupling parameters (S21, S31, S41) show slight variations, which are acceptable due to solver differences and port excitation handling as shown Figure 13(b). The axial ratio bandwidth in HFSS is approximately 1 GHz narrower than CST, yet still within the desired range as shown Figure 13(c). Gain values are generally consistent, with minor fluctuations of around 1 dB at certain frequencies as shown Figure 13(d). These variations are expected due to differences in meshing, boundary conditions, and solver algorithms.



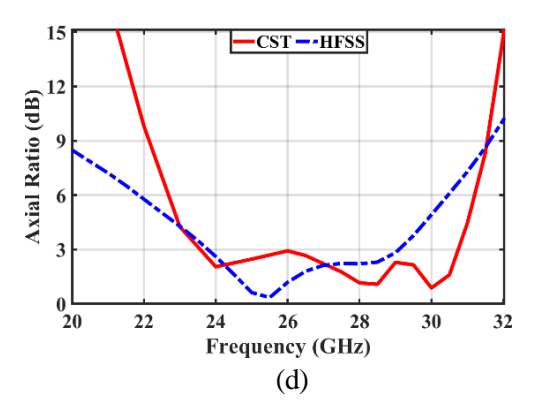


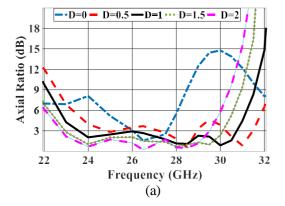
Fig. 13 Comparison of CST and HFSS simulation results for proposed four port MIMO antenna (a) S11 (dB), (b) Isolation (dB), (c) Gain (dBi), (d) Axial Ratio (dB).

3.2.1 Parametric analysis

In the parametric study, certain parameters significantly influence the efficiency of the MIMO system, such as D, which represents the distance between the antenna elements and parameter P2, denoting the vertical spacing between parasitic elements, as depicted in Figure 3.

A. Impact of D dimension

The impact of the D dimension, the distance between the elements, is crucial for the MIMO system's circular polarization efficacy. While this parameter has a minor effect on the S-parameters, it affects the axial ratio and characteristics. When varying D from 0 to 2 millimeters, observations from Figure 14(a) reveal that with D at zero, the MIMO system is not circularly polarized due to the axial ratio exceeding -3 dB. As D increases, the axial ratio improves until D reaches 1mm, at which point a shift occurs in the axial ratio bandwidth towards lower frequencies, accompanied by a decrease in bandwidth. Therefore, the optimal result for the axial ratio is achieved at D equal 1mm. Additionally, this variation in D dimension influences the system's gain, with the highest gain (8.54 dBi) observed at D of 1mm as shown Figure 14(b).



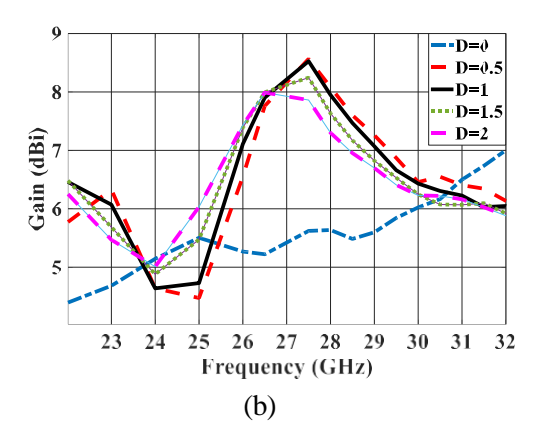


Fig. 14 Impact of D dimension on (a) AR (dB), and (b) Gain (dBi).

B. Impact of P2 dimension

In the parametric study, the variation of parameter P2 between parasitic elements has a minor impact on the S-parameters. When altering P2 from 0.15 to 0.55 for optimal results, observations from Figure 15(a) indicate that the axial ratio deteriorates at P2 starts to decline with further increases in P2. Regarding the gain, the influence of P2 is notable, with the gain improving from 7.8 to 8.54 dBi as P2 varies. The highest gain is achieved when P2 equals 0.45 millimeters, as illustrated in Figure 15(b). These findings underscore the significance of parameter P2 in optimizing both the axial ratio and gain characteristics of the MIMO antenna system equal 0.45mm.

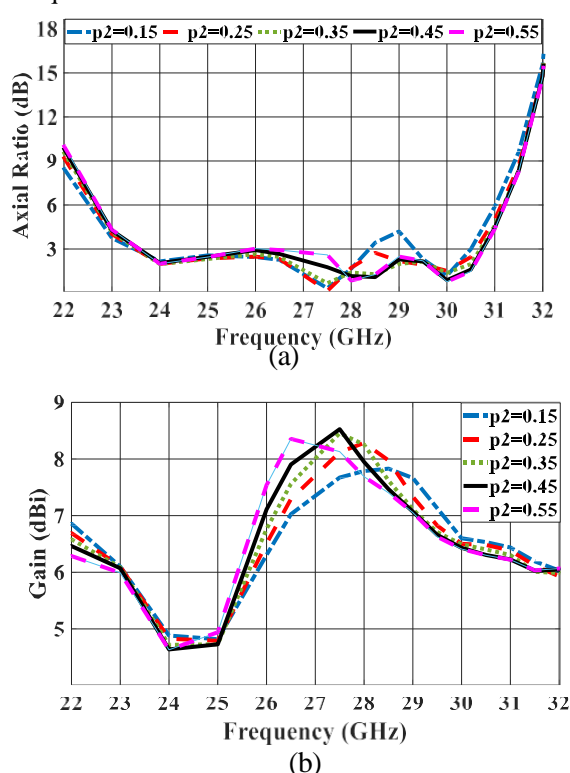


Fig. 15 Impact of P2 dimension on (a) AR (dB), and (b) Gain (dBi).

3.3 Wideband CP Eight-Port MIMO

In this section, an eight-element MIMO antenna system was developed, as depicted in Figure 5. The antenna elements were strategically arranged to achieve optimal performance in terms of bandwidth, gain, and isolation. Structural modifications were applied to the monopole ground, and interconnections were established between the ground planes to enhance the electromagnetic behavior of the system.

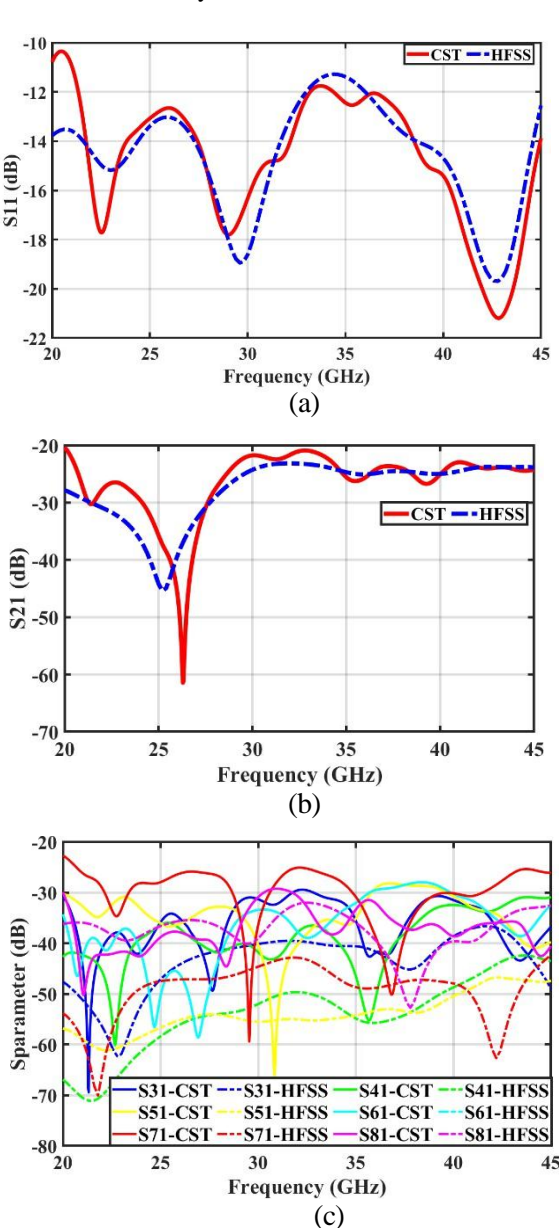
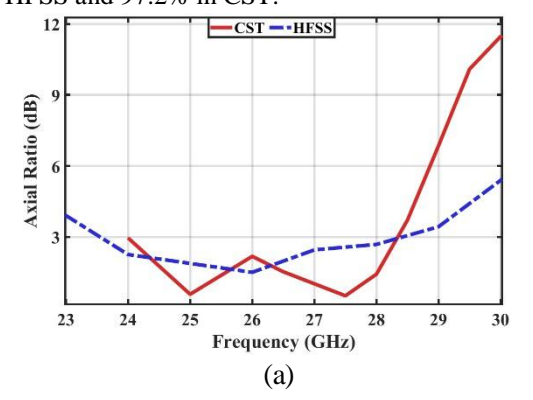


Fig. 16 Comparison of CST and HFSS simulation results for proposed eight port MIMO antenna (a) S11 (dB), (b) S21 (dB), and (c) Isolation (dB)

To verify the consistency of the results across different solvers, the eight-element CP MIMO antenna was simulated using both CST and HFSS. Figure 16(a) shows the return loss (S11), demonstrating excellent agreement between both tools, with a -10 dB impedance bandwidth of 20 to 45 GHz. The mutual coupling (S21) shown in Figure 16(b) remains below -20 dB across the frequency band, with HFSS yielding slightly better values. As depicted in Figure 16(c), the isolation levels between port 1 and the other ports (S31 to S81) show larger variation, these differences may stem from solver-specific field treatments and mesh refinement in large-scale arrays. HFSS predicts better isolation in several paths, whereas CST results show degradation, with isolation in all paths exceeding -25 dB, which is good. The axial ratio, displayed in Figure 17(a), shows better performance in HFSS with a 3 dB AR bandwidth of 23.5 to 28.4 GHz, compared to 24-28.3 GHz in CST. The gain comparison in Figure 17(b) indicates close agreement, with peak values of 8.62 dB in CST and 8.3 dB in HFSS. Lastly, Figure 18 presents the total radiation efficiency, where both tools achieve high performance, with maximum values of 96.2% in HFSS and 97.2% in CST.



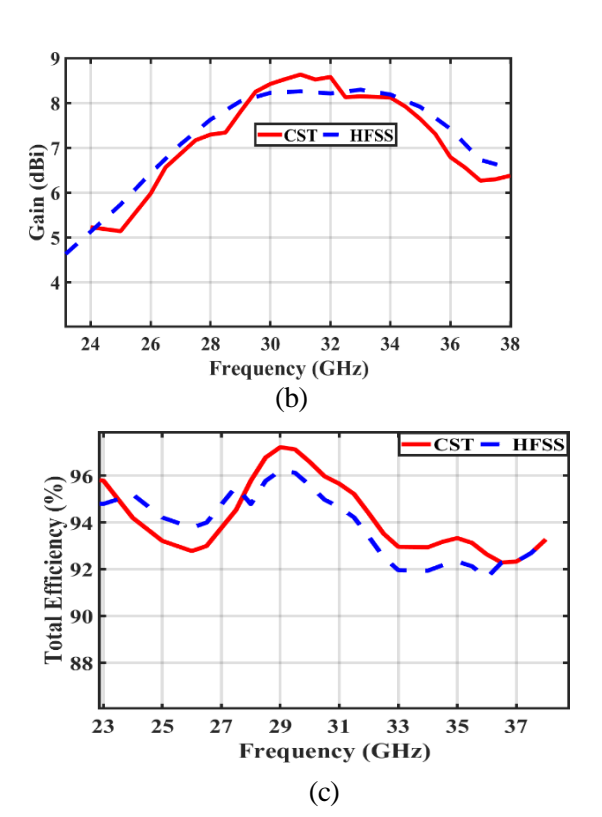


Fig. 17 Comparison of CST and HFSS simulation results for proposed eight port MIMO antenna (a) AR (dB) (b) Gain (dBi) (c) Total efficiency (%)

Table 3 Comparison the proposed four-port MIMO with other related work

Ref	Size mm ³	Bandwidth (GHz)	ARBW (dB)	Gain (dBi)	Isolation (dB)	No Ports
[37]	27.5 x 30 x 0.254	25.41 - 31.18	25.49 - 29.52	7.27	-25	2
[38]	23×18	26 - 40	Not CP	6.6	-18	4
[39]	Not given	25.6 - 32.4	26 - 26.5	6.1	-15	4
[40]	7.5 x 6 x 0.8	36.0 - 40.0	37.53 - 39.0	7.2	-20	2
	2 layer					
[41]	$20\times16.5\times0.99$	24.5 - 29.5	Not CP	8.81	-16.2	3
	2 layer					
Our work	31 x 25 x 1.575	21.3 - 45	23.5 - 30.7	8.5	-20	4

Table 3 presents a comparative analysis between the proposed MIMO antenna system and previously reported designs. It is evident that the proposed design offers significant improvements in several key performance metrics. Notably, our work achieves the widest impedance bandwidth, ranging from 21.3 GHz to 45 GHz, which surpasses all referenced designs. Additionally, it provides a broader axial ratio bandwidth (ARBW) of 23.5 GHz to 30.7 GHz, indicating superior circular polarization performance compared to most of the prior works. In terms of gain, the proposed antenna attains a high value of 8.5 dBi, which is among the highest reported. Furthermore, the design maintains a strong isolation performance below -20 dB for a four-port configuration. Therefore, the proposed MIMO antenna demonstrates a well-balanced performance, making it a strong candidate for next-generation high-frequency wireless communication systems.

References

- [1] 5G Americas. Understanding Millimeter Wave Spectrum for 5G Networks. Available online: https://www.5gamericas.org/ understanding-millimeter-wave-spectrum- for-5g-networks/ (accessed on 2 March 2025).
- [2] Ullah R, Ullah S, Faisal F, et al. A novel multi-band and multi-generation (2G, 3G,4G, and 5G) 9-elements MIMO antenna system for 5G smartphone applications. Wireless Networks 2021; 27: 4825–4837.
- [3] Wu D, Wang J, Cai Y, et al. Millimeterwave multimedia communications: challenges, methodology, and applications. IEEE Communications Magazine 2015; 53:
- [4] Ford R, Zhang M, Mezzavilla M, et al. Achieving Ultra-Low Latency in 5G Millimeter Wave Cellular Networks. IEEE Communications Magazine 2017; 55: 196–203.
- [5] Johnson JE, Shay O, Kim C, et al. Wearable Millimeter-Wave Device for Contactless Measurement of Arterial Pulses. IEEE Trans Biomed Circuits Syst 2019; 13: 1525–1534.
- [6] Bevacqua MT, Di Meo S, Crocco L, et al. Millimeter-Waves Breast Cancer Imaging via Inverse Scattering Techniques. IEEE J Electromagn RF Microw Med Biol 2021; 5: 246–253.
- [7] Mazaheri MH, Ameli S, Abedi A, et al. A millimeter wave network for billions of things. In: Proceedings of the ACM Special Interest Group on Data Communication. New York, NY, USA: Association for Computing Machinery, pp. 174–186.
- [8] Qingling Z, Li J. Rain Attenuation in Millimeter Wave Ranges. ISAPE 2006
 - 2006 7th International Symposium on Antennas, Propagation and EM Theory,

4. Conclusion

This study presents a new design for a wideband circularly polarized millimeter-wave MIMO antenna, four-port demonstrating enhanced performance across critical parameters. The antenna achieves high bandwidth, 3-dB impedance axial ratio bandwidth, and maintains high isolation levels. An extended MIMO architecture with eight elements was developed, achieving a total efficiency exceeding 97%. Future work will focus on optimization and isolation techniques. Moreover, the development of a larger-scale massive MIMO system comprising more than eight elements is planned, aiming to address the growing demands of next-generation wireless communication systems and 5G millimeterwave applications.

Proceedings; 2006. Epub ahead of print April 2006. DOI:10.1109/ISAPE.2006.353538.

- [9] Sulyman AI, Nassar AT, Samimi MK, et al. Radio propagation path loss models for 5G cellular networks in the 28 GHZ and 38 GHZ millimeter-wave bands. IEEE Communications Magazine 2014; 52: 78–86.
- [10] Samimi MK, Rappaport TS, MacCartney GR. Probabilistic Omnidirectional Path Loss Models for Millimeter-Wave Outdoor Communications. IEEE Wireless Communications Letters 2015; 4: 357–360
- [11] Ibrahim Nawar R, Yahia Hassan A, Mahmoud Abdelhady A. High gain wideband circularly polarized antenna with modified ground plane. Indonesian Journal of Electrical Engineering and Computer Science 2023; 32: 284.
- [12] Miura Y, Hirokawa J, Ando M, et al. A circularly-polarized aperture array antenna with a corporate-feed hollow-waveguide circuit in the 60 GHz-band. 2011 IEEE International Symposium on Antennas and Propagation (APSURSI) 2011; 3029–3032.
- [13] Bisharat D, Liao S, Xue Q. High Gain and Low Cost Differentially Fed Circularly Polarized Planar Aperture Antenna for Broadband Millimeter-Wave Applications. IEEE Trans Antennas Propag 2015; 64: 1.
- [14] Aliakbari H, Abdipour A, Mirzavand R, et al. A single feed dual-band circularly polarized millimeter-wave antenna for 5G communication. In: 2016 10th European Conference on Antennas and Propagation (EuCAP). 2016, pp. 1–5.

- [15] Chen G-T, Gong Y-J, Chiu T. Millimeter-Wave Circularly Polarized Patch Antenna With Enhanced Axial-Ratio Bandwidth. In: 2021 IEEE International Symposium on Radio-Frequency Integration Technology (RFIT). 2021, pp. 1–2.
- [16] Al-Saedi H, Abdel-Wahab W, Gigoyan S, et al. Ka-Band Antenna With High Circular Polarization Purity and Wide AR Beamwidth. IEEE Antennas Wirel Propag Lett 2018; PP: 1.
- [17] Nawar RI, Abdelhady AM, Hassan AY. High Performance Circularly Polarized Quad-Elements for 5G Wireless Communications. Arab J Sci Eng. Epub ahead of print 2025. DOI: 10.1007/s13369-024-09844-3.
- [18] Sharawi MS. Printed Multi-Band MIMO Antenna Systems and Their Performance Metrics [Wireless Corner]. IEEE Antennas Propag Mag 2013; 55: 218–232.
- [19] Rahman M, NagshvarianJahromi M, Mirjavadi SS, et al. Compact UWB Band-Notched Antenna with Integrated Bluetooth for Personal Wireless Communication and UWB Applications. Electronics (Basel); 8. Epub ahead of print 2019. DOI: 10.3390/electronics8020158.
- [20] Ojaroudi Parchin N, Jahanbakhsh Basherlou H, Alibakhshikenari M, et al. Mobile-Phone Antenna Array with Diamond-Ring Slot Elements for 5G Massive MIMO Systems. Electronics (Basel); 8. Epub ahead of print 2019. DOI: 10.3390/electronics8050521.
- [21] Munir ME, Nasralla MM, Esmail MA. Four port tri-circular ring MIMO antenna with wide-band characteristics for future 5G and mmWave applications. Heliyon; 10. Epubahead of print 30 April 2024. DOI: 10.1016/j.heliyon.2024.e28714.
- [22] Saad A, Mohamed H. Printed Millimeter- Wave MIMO-Based Slot Antenna Arrays for 5G Networks. AEU International Journal of Electronics and Communications; 99. Epub ahead of print April 2018.

 DOI:

10.1016/j.aeue.2018.11.029.

- [23] Park J-S, Ko J-B, Kwon H-K, et al. A Tilted Combined Beam Antenna for 5G Communications Using a 28-GHz Band. IEEE Antennas Wirel Propag Lett 2016; 15: 1.
- [24] Shoaib N, Shoaib S, Khattak RY, et al. MIMO Antennas for Smart 5G Devices. IEEE Access 2018; 6: 77014–77021.
- [25] Sipal D, Abegaonkar M, Koul S. Easily Extendable Compact Planar UWB MIMO Antenna Array. IEEE Antennas Wirel Propag Lett 2017; PP: 1.
- [26] Liu X, Wang Z, Yin Y-Z, et al. A compact ultrawideband MIMO antenna using QSCA for high isolation.

- Antennas and Wireless Propagation Letters, IEEE 2014; 13: 1497– 1500.
- [27] Mao C, Chu Q-X. Compact coradiator UWB-MIMO antenna with dual polarization. Antennas and Propagation, IEEE Transactions on 2014; 62: 4474–4480.
- [28] Desai A, Patel J, Upadhyaya T. Compact Wideband Four Element Optically Transparent MIMO Antenna for mm-Wave 5G Applications. IEEE Access; 8. Epub ahead of print April 2020. DOI: 10.1109/ACCESS.2020.3033314.
- [29] Akbari M, Abo Ghalyon H, Farahani M, et al. Spatially Decoupling of CP Antennas Based on FSS for 30-GHz MIMO Systems. IEEE Access 2017; 5: 6527–6537.
- [30] Hussain N, Jeong M-J, Park J, et al. A Broadband Circularly Polarized Fabry-Perot Resonant Antenna Using A Single- Layered PRS for 5G MIMO Applications. IEEE Access 2019; 7: 42897–42907.
- [31] Liu Z, LU W-B. Low-Profile Design of Broadband High Gain Circularly Polarized Fabry-Perot Resonator Antenna and its Array with Linearly Polarized Feed. IEEE Access 2017; PP: 1.
- [32] Xu M, Zhang J. Circularly Polarized Multiple-Input Multiple-Output Dielectric Resonator Antenna for 5G Millimeter- Wave Application. Electronics (Basel); 12. Epub ahead of print 2023. DOI: 10.3390/electronics12204258.
- [33] Chen HN, Song J-M, Park J-D. A Compact Circularly Polarized MIMO Dielectric Resonator Antenna Over Electromagnetic Band-Gap Surface for 5G Applications. IEEE Access 2019; PP: 1.
- [34] Chandrashekar A, Singh V, Dwivedi A, et al. Metasurface inspired printed dual-port MIMO antenna system with LP to CP conversion features for millimeter wave n260 band applications. Sci Rep; 14. Epub ahead of print April 2024. DOI: 10.1038/s41598-024-75696-4.
- [35] Ibrahim AA, Ali WAE. High gain, wideband and low mutual coupling AMC- based millimeter wave MIMO antenna for 5G NR networks. AEU International Journal of Electronics and Communications; 142. Epub ahead of print

 1 December 2021. DOI:
 - 1 December 2021. DOI: 10.1016/j.aeue.2021.153990.
- [36] Balanis, C.A. (2016). Antenna Theory: Analysis and Design. 4th ed. Hoboken, New Jersey Wiley, pp.814–823. Chapter 14.3 Circular Patch.

- [37] Xu M, Zhang J. Circularly Polarized Multiple-Input Multiple-Output Dielectric Resonator Antenna for 5G Millimeter- Wave Application. Electronics (Basel); 12. Epub ahead of print 2023. DOI: 10.3390/electronics12204258.
- [38] Munir ME, Nasralla MM, Esmail MA. Four port tri-circular ring MIMO antenna with wide-band characteristics for future 5G and mmWave applications. Heliyon; 10. Epub ahead of print 30 April 2024. DOI: 10.1016/j.heliyon.2024.e28714.
- [39] Modak S, Farooq U, Lokam A. Circularly Polarized MIMO Antenna System for Millimeter Wave 5G Applications Using Characteristic Mode Theory. International Journal of Communication Systems 2025; 38: e70017.
- [40] C A, Singh V, Dwivedi AK, et al. Metasurface inspired printed dual-port MIMO antenna system with LP to CP conversion features for millimeter wave n260 band applications. Sci Rep 2024; 14: 24437.
- [41] Hamlbar Gerami H, Kazemi R, Fathy AE. Design and Implementation of a Compact

Dual-Band MIMO Antenna Module With Enhanced Bandwidth and Isolation. International Journal of RF and Microwave Computer-Aided Engineering 2025; 2025: 7326700.